ARMY RESEARCH LABORATORY

Structure Function Spectra and Acoustic Scattering Due to Homogeneous Isotropic Atmospheric Turbule Ensembles

by George H. Goedecke, Michael DeAntonio, and Harry J. Auvermann

ARL-TR-1518

August 1998

Army Research Laboratory
Adelphi, MD 20783-1197

ARL-TR-1518 **August 1998**

Structure Function Spectra and Acoustic Scattering Due to Homogeneous Isotropic Atmospheric Turbule Ensembles

George H. Goedecke and Michael DeAntonio
New Mexico State University
Department of Physics
Las Cruces, NM 88003-8001

Harry J. Auvermann
Information Science and Technology Directorate, ARL

Abstract

Expressions are derived for the spectral densities $\Phi^T(K), \Phi^v_{ij}(K)$ of the temperature and velocity structure functions of atmospheric turbulence, and for the corresponding Born approximation far-field acoustic scattering cross-sections, due to homogeneous isotropic stationary ensembles of self-similar localized turbules having many different scale lengths. It is shown that for some range $K_{\min} \leq K \leq K_{\max}$, the "inertial range," the spectral densities obey power laws with dependence K^{-P_T}, K^{-P_v}. The exponents (P_T, P_v) depend only on choices of scaling relations and are independent of turbule morphology. Only $K_{\min}, K_{\max}$, and the values of the spectral densities outside the inertial range are morphology-dependent. Expressions for $K_{\min}$ and $K_{\max}$ are derived in terms of inner and outer scale lengths in the turbule ensemble. If the turbule scale lengths a_α are chosen to be in geometric sequence ($a_{\alpha+1}/a_\alpha$ = constant independent of α), and if the power law is given as $P_T = P_v = 11/3$, the Kolmogorov spectrum in the inertial range, then not only must the turbule velocity and temperature amplitudes scale as $a_\alpha^{1/3}$, the usual result, but also the turbule packing fractions must be independent of scale length. Expressions for the structure parameters (C_T^2, C_v^2) that occur in the usual Kolmogorov spectra are obtained in terms of the turbule model parameters. It is also shown that quasi-Gaussian spectra result for the choice $P_T = P_v = 0$ and Gaussian turbule morphology.

Contents

Figures

1. Introduction

This is the second in a series of technical reports that examine a turbule model of atmospheric turbulence and the acoustic scattering predicted by the model. The previous report [1] laid the groundwork for this and succeeding reports in the series. In Goedecke et al [1], the general properties of the Born approximation far-field acoustic scattering predicted by Monin's equation [2] were obtained. In addition, expressions for the acoustic scattering amplitudes and cross-sections were derived for individual model turbules of a given scale length and for their orientational averages, and it was shown that an ensemble of randomly oriented turbules of arbitrary morphology may be replaced by an equivalent ensemble of spherically symmetric nonuniformly rotating turbules, with randomly directed rotation axes.

In this report, we connect the turbule model predictions to the structure function predictions for the case of isotropic homogeneous fully developed steady-state atmospheric turbulence. This is an essential step toward the ultimate goal of describing acoustic propagation and scattering in inhomogeneous anisotropic turbulence using a turbule model. In section 2, we construct an ensemble of self-similar turbules of many different scale lengths, each with random location in a bounded volume V and with random orientation. We adopt general scaling laws in which the number of turbules of a given scale length a_α and their velocity and temperature variation amplitudes scale according to powers of a_α, and in which the spectrum of scale lengths follows a general power law that includes the usual fractal geometric sequence in which $a_{\alpha+1}/a_\alpha$ is independent of a_α. We also show that a kinetic energy cascade model similar to that of Kolmogorov yields one connection among the scaling exponents. We develop expressions for the spectral densities $\Phi^T(K), \Phi^v_{ij}(K)$ of the temperature and velocity structure functions in terms of these turbule model parameters. We show that a power law scattering spectrum generally exists for some range $K_{\min} \leq K \leq K_{\max}$, the "inertial range," in which the cross-sections each depend on K to some power that could be different for the temperature than for the velocity scattering. We also show that the power laws are independent of turbule morphology, and that only $K_{\min}$ and $K_{\max}$ and the behavior of the spectral densities for K outside the inertial range are morphology dependent. We derive expressions for $(K_{\min}, K_{\max})$ in terms of the inner and outer scale length of the ensemble, and the characteristic widths of the spectral densities of individual turbules. We show that, if we wish to obtain a spectrum in which both spectra depend on $K^{-11/3}$ in the inertial range, then for the fractal sequence only, not only must the velocity and temperature amplitudes scale as $a_\alpha^{1/3}$, the usual result, but also the turbule packing fractions must be scale-invariant. We show that a Gaussian scattering spectrum requires quite different scaling exponents than a $K^{-11/3}$ spectrum. We also obtain expressions in terms of the turbule ensemble parameters for the structure parameters (C_T^2, C_v^2) that occur in the Kolmogorov structure functions. We investigate the specific behavior of the spectral densities versus K for two example turbule structures.

In section 3, we express the Born approximation far-field cross-sections as functions of scattering angle θ for acoustic scattering by the velocity and temperature fluctuations of the turbulence derived in section 2, and show under what conditions the cross-sections deviate appreciably from a power law dependence on $\sin(\theta/2)$.

Finally, in section 4 we summarize and discuss our results and plans for further work.

2. Turbule Model of Homogeneous Isotropic Steady-State Atmospheric Turbulence

2.1 Model Turbules

We model turbulence contained in a volume V_s as an ensemble of self-similar stationary localized turbules of different scale lengths. On the average, in V_s we allow N_α turbules of scale length a_α, $\alpha = (1, N_s)$, where N_s is the total number of different scale lengths in the ensemble, so that $N = \Sigma_\alpha N_\alpha$ is the total ensemble average number of turbules in V_s, in steady state. We assume in this report that the a_α are much smaller than the scale length a_s of the volume V_s.

We take a_1 as the largest scale length in the ensemble, and a_{N_s} as the smallest; these lengths define the outer and inner scales of the turbulence, respectively. Each turbule is characterized by the general scalable static temperature variation and solenoidal velocity fields $(\Delta T_0(\mathbf{r}), \mathbf{v}_0(\mathbf{r}))$ chosen in the previous report in this series [1]. For turbule number n, we have

$$\mathbf{v}_{0n}(\mathbf{r}) = \boldsymbol{\nabla}_{\xi_n} \times \mathbf{A}_n(\boldsymbol{\xi}_n), \qquad \Delta T_{0n}(\mathbf{r}) = T_n(\boldsymbol{\xi}_n) \tag{1}$$

where

$$\boldsymbol{\xi}_n = (\mathbf{r} - \mathbf{b}_n)/a_n, \tag{2}$$

$\mathbf{b}_n$ is the "location" of the turbule, i.e., the point about which the turbule is localized, and $\mathbf{A}_n(\boldsymbol{\xi}_n)$ is an unrestricted vector field.

For convenience, we allow uncorrelated locations $\mathbf{b}_n$. This means that the joint probability distribution for the locations of the N turbules may be written as

$$P(\mathbf{b}_1, \ldots, \mathbf{b}_N) = p_1(\mathbf{b}_1) \ldots p_N(\mathbf{b}_N), \tag{3}$$

the product of N one-particle distributions, with

$$\int d^3 b p_n(\mathbf{b}) = 1, \qquad \text{all } n. \tag{4}$$

We also want the turbulence to be homogeneous. This means that the ratios of the number densities of turbules of different scale lengths should be independent of position in V_s; this requires

$$p_n(\mathbf{b}) = p(\mathbf{b}), \tag{5}$$

independent of n. If we also want the turbulence to be uniform in V_s, then we must choose

$$\begin{aligned} p(\mathbf{b}) &= V_s^{-1}, \mathbf{b}\epsilon V_s \\ &= 0, \text{ otherwise.} \end{aligned} \tag{6}$$

An isotropic ensemble consists of randomly oriented copies of turbules of arbitrary morphology for each scale length, and is thus characterized by spherically symmetric envelope functions $\tilde{B}_T^2, \tilde{B}_v^2$ as defined by Goedecke et al [1], namely,

$$\left\langle |\tilde{T}_n(\mathbf{K}a_n)|^2 \right\rangle = \pi^3(\delta T_\alpha)^2 \tilde{B}_T^2(Ka_\alpha) \tag{7}$$

$$\left\langle \tilde{A}_{ni}(\mathbf{K}a_n) \right\rangle = 0 \tag{8}$$

$$\left\langle \tilde{A}_{ni}\tilde{A}_{nj}^*(\mathbf{K}a_n) \right\rangle = \tfrac{1}{3}\pi^3 \delta_{ij} v_\alpha^2 \tilde{B}_v^2(\mathbf{K}a_\alpha). \tag{9}$$

The $\tilde{T}_n(\mathbf{y}_n)$ and $\tilde{A}_{ni}(\mathbf{y}_n)$ are the Fourier transforms of $T_n(\boldsymbol{\xi}_n)$ and $A_{ni}(\boldsymbol{\xi}_n)$, respectively, as defined by Goedecke et al [1], namely,

$$\tilde{T}_n(y) \equiv \int d^3\xi e^{-i\boldsymbol{\xi}\cdot\mathbf{y}} T_n(\boldsymbol{\xi}), \qquad \tilde{\mathbf{A}}_n(y) \equiv \int d^3\xi e^{-i\boldsymbol{\xi}\cdot\mathbf{y}} \mathbf{A}_n(\boldsymbol{\xi}), \tag{10}$$

where the integrals are extended over all $\boldsymbol{\xi}$-space, since the individual turbules are localized and their scale lengths a_n are assumed to be much smaller than the scale length a_s of V_s. Here, the expectation involves averaging over random orientations, so the amplitudes $(\delta T_a, v_\alpha)$ and the argument of the envelope functions depend only on the scale length index α. The envelope functions themselves are independent of α; that is, they are the same functions of their arguments for all α. This provides self-similarity. The factors of π^3 and $1/3$ are inserted for convenience as in Goedecke et al [1].

2.2 Scaling

In order to describe the complete ensemble, we assume that the quantities $(N_\alpha, \delta T_\alpha, v_\alpha)$ scale with a_α. We put

$$\frac{N_\alpha}{N_1} = \left(\frac{a_\alpha}{a_1}\right)^{-\beta}, \ \left(\frac{\delta T_\alpha}{\delta T_1}\right) = \left(\frac{a_\alpha}{a_1}\right)^{\gamma}, \left(\frac{v_\alpha}{v_1}\right) = \left(\frac{a_\alpha}{a_1}\right)^{\nu}, \tag{11}$$

where (β, γ, ν) are parameters. In addition, we must decide how to relate the scale lengths to the index α. One relation that has been used is [3]

$$a_\alpha = a_1 e^{-\mu(\alpha-1)}, \quad \mu > 0, \tag{12}$$

where μ is a parameter that is determined by N_s, the number of scale lengths, and the ratio (a_{N_s}/a_1) of inner to outer scale lengths:

$$\mu = -(N_s - 1)^{-1} \ln m, \quad m \equiv a_{N_s}/a_1. \tag{13}$$

Equation (12) implies that the scale lengths form a geometric sequence, in which

$$a_2/a_1 = a_3/a_2 = \ldots = e^{-\mu};$$

that is, the ratio of successively smaller scale lengths is a constant whose value lies between zero and unity. This is a kind of fractal scaling [3].

A general power law scaling relation is given by

$$a_\alpha = a_1(1 + q\mu(\alpha - 1))^{-1/q}, \quad q > 0, \quad \mu > 0, \tag{14}$$

where here μ is determined in terms of (m, q) by

$$\mu = q^{-1}(m^{-q} - 1)/(N_s - 1). \tag{15}$$

Equations (14) and (15) actually reduce to equations (12) and (13) respectively, when q goes to 0; so in what follows we may use just equations (14) and (15), with $q \geq 0$. We will also make use of the Kolmogorov concept of energy transfer in fully developed (steady-state) turbulence, in which energy is provided to the ensemble at the largest or outer scale. The largest eddies continually form but are unstable because of their large Reynolds numbers, and thereby continually fragment into smaller eddies, which in turn fragment further, etc. This cascade continues down to eddies of a size small enough to be stable, that is, to eddies whose Reynolds numbers are of order unity. These smallest or inner scale eddies dissipate almost all the energy that is being input at the largest scale. In steady state, all the ensemble average quantities $(N_\alpha, v_\alpha, \delta T_\alpha)$, and the relationships like equations (12) or (14), are constant in time. By dimensional analysis and from the fluid equations, the kinetic energy transfer rate $\dot{\mathcal{E}}_{K\alpha}$ from turbules of scale length a_α to the next smaller is

$$\dot{\mathcal{E}}_{K\alpha} = (C)(N_\alpha)(a_\alpha^3)(\delta T_\alpha)(v_\alpha^2/a_\alpha), \tag{16}$$

where C is a constant with dimension of reciprocal volume. That is, the energy transfer rate is proportional to the number of turbules of size a_α in V, the volume of each, the kinetic energy per unit mass $v_\alpha^2/2$ of each, and the characteristic rate of transfer v_α/a_α. The Kolmogorov model consists of neglecting dissipation in all eddies except the smallest. This means that, in steady state, $\dot{\mathcal{E}}_{K\alpha}$ is independent of α, for $\alpha = (1, N_s - 1)$. Using equation (11) in this model then yields one ratio among the parameters (β, ν):

$$\beta = 3\nu + 2. \tag{17}$$

In the atmosphere, the ratios $|\Delta T_0|/T_\infty$ and v_0/c_∞ are usually of the same order. This implies that our turbule temperature variation amplitudes δT_α should be proportional to v_α, whereby we get directly from equation (11)

$$\gamma = \nu. \tag{18}$$

On the other hand, if we apply the Kolmogorov energy cascade model to the thermal energy constant of the turbules in our ensemble, we get for the thermal energy transfer rate $\dot{\mathcal{E}}_{T\alpha}$ from turbules of one scale length to the next smaller

$$\dot{\mathcal{E}}_{T\alpha} = (C')(N_\alpha)(a_\alpha^3)(\delta T_\alpha)(v_\alpha/a_\alpha), \tag{19}$$

where C' is a constant. This says that the energy transfer rate is proportional to the thermal energy content of a turbule, which is proportional to δT_α. If we require this rate to be independent of a, then we get from equations (11) and (14)

$$\gamma = 2\nu. \tag{20}$$

This is equivalent to stating that δT_α is proportional to v_α^2. We see in the next section that these two possibilities of equations (18) and (20) yield quite different behavior for the velocity and temperature variation structure functions of the ensemble.

2.3 Structure Function Spectra

2.3.1 General

The velocity and temperature variation structure functions are important quantities that characterize atmospheric turbulence [4,5]. In this section, we obtain formulas for the spectral densities of these structure functions from our turbule model, for isotropic homogeneous turbulence.

The temperature variation and velocity fields of the turbulence in V_s are just the superposition of those of the localized turbules in V_s:

$$\Delta T_0(\mathbf{r}) = \sum_n \Delta T_{0n}(\mathbf{r}), \qquad v_0(\mathbf{r}) = \sum_n v_{0n}(\mathbf{r}). \tag{21}$$

We are interested in the Fourier transforms

$$\Delta\tilde{T}_0(\mathbf{K}) \equiv \int_{V_s} d^3r e^{-i\mathbf{K}\cdot\mathbf{r}} \Delta T_0(\mathbf{r}), \qquad \tilde{v}_0(\mathbf{K}) \equiv \int_{V_s} d^3r e^{-i\mathbf{K}\cdot\mathbf{r}} \mathbf{v}_0(\mathbf{r}). \tag{22}$$

Specifically, we wish to obtain general expressions for the spectral densities

$$\Phi^T(K) \equiv \left\langle |\Delta T_0(\mathbf{K})|^2 \right\rangle, \qquad \Phi_{ij}^v(\mathbf{K}) = \left\langle \tilde{v}_{0i}(\mathbf{K})\, \tilde{v}_{0j}^*(\mathbf{K}) \right\rangle, \tag{23}$$

where the expectations $\langle\rangle$ imply averaging over random turbule locations b and random turbule orientations, as discussed in section 2.1 above.

Combination of equations (1), (2), (10), (21), and (22) yields

$$\tilde{v}_0(\mathbf{K}) = i \sum_n e^{-i\mathbf{K}\cdot\mathbf{b}_n} a_n^4 \mathbf{K} \times \tilde{A}_n(\mathbf{K}a_n) \tag{24}$$

$$\Delta\tilde{T}_0(\mathbf{K}) = \sum_n e^{-i\mathbf{K}\cdot\mathbf{b}_n} a_n^3 \tilde{T}_n(\mathbf{K}a_n). \tag{25}$$

The spectral densities of equation (23) are then

$$\begin{aligned}\Phi^T(\mathbf{K}) &= \sum_n a_n^6 \left\langle |\tilde{T}_n(\mathbf{K}a_n)|^2 \right\rangle \\ &\quad + |\tilde{p}(\mathbf{K})|^2 \sum_n a_n^3 \left\langle \tilde{T}_n(\mathbf{K}a_n) \right\rangle \sum_{\ell \neq n} a_\ell^3 \left\langle \tilde{T}_\ell^*(\mathbf{K}a_n) \right\rangle \end{aligned} \tag{26}$$

$$\Phi_{ij}^v(\mathbf{K}) = \epsilon_{ipq}\epsilon_{jrs} K_p K_r \sum_n a_n^8 \left\langle \tilde{A}_{nq}(\mathbf{K}a_n) \tilde{A}_{ns}^*(\mathbf{K}a_n) \right\rangle, \tag{27}$$

where equation (8) was used. Here ϵ_{ipq} is the Levi-Civita symbol, and

$$\tilde{p}(\mathbf{K}) = \int_{V_s} d^3b e^{-i\mathbf{K}\cdot\mathbf{b}} p(\mathbf{b}) \tag{28}$$

is the Fourier transform of the "one-particle" location distribution of equation (6).

In the standard treatment [4], the mean temperature in V_s is assumed equal to the remote reference temperature T_∞, or $\int_{V_s} d^3r \Delta T_0(\mathbf{r}) = 0$. We will assume that here, in order to facilitate comparisons of our turbule model spectra with the commonly used spectra. For simplicity we assume that in the ensemble,

$$\left\langle \tilde{T}_n(\mathbf{K}a_n) \right\rangle = \pm \pi^{3/2} \delta T_\alpha \tilde{B}_T(\mathbf{K}a_\alpha) = \pm \left\langle |\, \tilde{T}_n(\mathbf{K}a_n)|^2 \right\rangle^{\frac{1}{2}}, \tag{29}$$

with equal numbers having the $(+,-)$ signs. This ensures that $\int_{V_s} d^3r \Delta T_0(\mathbf{r}) = 0$. It also takes advantage of the result of Goedecke et al [1], that an isotropic ensemble of a given scale length may often be replaced by an ensemble of spherically symmetric turbules. For such turbules with a positive definite envelope function, equation (29) automatically would be valid. With this assumption, we have

$$\sum_n a_n^3 \left\langle \tilde{T}_n(\mathbf{K}a_n) \right\rangle = 0. \tag{30}$$

Then, from equations (7), (9), and (26) to (30), we get

$$\begin{aligned} \Phi^T(\mathbf{K}) &= \left(1 - |\, \tilde{p}(\mathbf{K})|^2\right) \pi^3 \sum_n N_\alpha (\delta T_\alpha)^2 a_\alpha^6 \tilde{B}_T^2(\mathbf{K}a_\alpha) && (31) \\ \Phi_{ij}^v(\mathbf{K}) &= (\delta_{ij} - \hat{K}_i \hat{K}_j)(\pi^3/3) \sum_n N_\alpha v_\alpha^2 a_\alpha^6 (\mathbf{K}a_\alpha)^2 \tilde{B}_v^2(\mathbf{K}a_\alpha). && (32) \end{aligned}$$

Note that the sums over turbules in equations (26) and (27) are replaced by sums over size index α in equations (31) and (32), with N_α included.

The factor involving $|\, \tilde{p}(\mathbf{K})|^2$ in equation (31) comes from writing $\sum_n \sum_{\ell \neq n} = \sum_n \sum_\ell - \sum_n$ in the second term of equation (26), and using equations (29) and (30). In general, if $\int_{V_s} d^3r \Delta T_0(\mathbf{r}) = 0$, then $\Phi^T(\mathbf{K} = 0)$ must be zero; the factor $(1 - |\, \tilde{p}(\mathbf{K})|^2)$ in equation (31) ensures this, since $\tilde{p}(\mathbf{K} = 0) = 1$, because $p(\mathbf{b})$ is a probability density (see eq. (28)).

It is important to note that $\tilde{p}(\mathbf{K})$ is extremely small except for K near zero. For example, suppose that V_s is a spherical volume of radius a_s centered at the origin. Then, from equations (6) and (28)

$$\tilde{p}(\mathbf{K}) = 3(Ka_s)^{-3} \left[\sin Ka_s - Ka_s \cos Ka_s\right]. \tag{33}$$

Thus for large Ka_s, $|\tilde{p}(\mathbf{K})|^2$ is smaller than $(Ka_s)^{-4} << 1$. Therefore, in the spectral density $\Phi^T(K)$, the $|\tilde{p}(\mathbf{K})|^2$ factor may be dropped out, except for very small K such that $Ka_s \leq 1$. But its presence is essential in order to comply with the assumption that $\int_{V_s} d^3r \Delta T_0(\mathbf{r}) = 0$.

This assumption is not necessary; if it is not made, then the spectrum $\Phi^T(K)$ will have a different behavior for $K \to 0$ than that of equation (31). We will investigate this in a later report.

Note that the velocity spectrum $\Phi^v_{ij}(\mathbf{K})$ includes the factor of $(\delta_{ij} - \hat{K}_i\hat{K}_j)$, characteristic for solenoidal velocities [4]. Also note that, for the bounded envelope functions $\tilde{B}^2_v$ that will be used, the factor $(Ka_\alpha)^2$ ensures that $\Phi^v_{ij}(K \to 0) \to 0$, which is also a requirement for solenoidal velocities, directly related to the results of Goedecke et al [1] and Monin [2] that forward acoustic scattering due to such turbulent velocities is zero.

2.3.2 Inclusion of Scaling

In what follows, we replace the sum over size index α by an integral. This will be valid if the number of different scale lengths in the ensemble is large, as we shall assume. We then write

$$\sum_{\alpha=1}^{N_s} = \int_1^{N_s} d\alpha = \int_{a_1}^{a_{N_s}} da/(da/d\alpha); \qquad da/d\alpha = \mu a_1^{-q} a^{1+q} \tag{34}$$

where the last equality results from equation (14).

From equations (31), (32), and (34) and the scaling relations (11) to (15), we then get the following expressions for the spectral densities:

$$\Phi^T(K) = (1 - |\tilde{p}(\mathbf{K})|^2)\,(\pi^3 N_1 (\delta T_1)^2 a_1^6/\mu) x^{-P_T} J^T_{P_T-1}(mx, x) \tag{35}$$

$$\Phi^v_{ij}(\mathbf{K}) = (\delta_{ij} - \hat{K}_i\hat{K}_j)(\pi^3 N_1 v_1^2 a_1^6/3\mu) x^{-P_v} J^v_{P_v+1}(mx, x), \tag{36}$$

where (m, μ) are defined by equations (13) to (15), and

$$x \equiv Ka_1; \tag{37}$$

$$J^{T,v}_s(mx, x) \equiv \int_{mx}^{x} dy\, y^s \tilde{B}^2_{T,v}(y) \tag{38}$$

$$P_T = 6 + 2\gamma - \beta - q, \qquad P_v = 6 + 2\nu - \beta - q. \tag{39}$$

Here $q \geq 0$; $q = 0$ corresponds to the fractal scaling of equation (11).

Thus the spectra of equations (35) and (36) depend on the integrals of the generic form of equation (38). It is important to determine qualitatively how these integrals depend on (s, m, x). In all cases, the envelope functions $\tilde{B}^2_{T,v}(y)$ go to zero rapidly for large y; otherwise, individual turbules would not be localized. Also, we expect the $\tilde{B}^2(y)$ to be bounded everywhere. Thus, if x is large, then $J_s(mx, x) \approx J_s(mx, \infty)$ to very good approximation, as long as the $\tilde{B}^2(y)$ go to zero faster than y^{-s-1} for large y. Similarly, if $mx << 1$, then $J_s(mx, x) \approx J_s(0, x)$ to very good approximation, as long as the $y^s \tilde{B}^2(y) \to y^t$, with $t > -1$, for $y \to 0$. Thus, in many cases, there will exist a range of x such that

$$J_s(mx, x) \approx J_s(0, \infty) = \text{ constant} \tag{40}$$

to a very good approximation.

For this range of x, equations (35) and (36) show that the spectra have a power law dependence on x and thus on K, with powers $(-P_T, -P_v)$. Conventional language defines this range of x or K as the "inertial range."

We note that, if the powers (P_T, P_v) are to be the same, then from equation (39), we must have equation (18),

$$\gamma = \nu, \tag{41}$$

which is what resulted from the discussion preceding equation (18), not from that preceding equation (21). We shall adopt $\gamma = \nu$. Then equations (17) and (39) yield

$$P = P_T = P_v = 4 - \nu - q. \tag{42}$$

2.3.3 Inertial Range Boundaries

The boundaries of the inertial range of x may be estimated as follows. The integrand $I_s(y)$ of $J_s(mx, x)$ of equation (38) is $y^2 \tilde{B}^2(y)$; for $s > 0$ and $\tilde{B}^2(y)$ that decrease monotonically faster than y^{-s} as y increases, it has a single maximum at $y = y_{sm}$ given by $I'_s(y_{sm}) = 0$, or

$$y_{sm} = -\tfrac{1}{2} s \tilde{B}(y_{sm}) / \tilde{B}'(y_{sm}). \tag{43}$$

The integrand has a characteristic width that also depends on s and the envelope function $\tilde{B}(y)$. We define $y_{s\pm}$ by requiring that $I_s(y_{s\pm})$ be some fraction of $I(y_{sm})$. In this report we choose

$$I_s(y_{s\pm}) = e^{-2} I_s(y_{sm}), \qquad y_{s-} < y_{sm} < y_{s+}. \tag{44}$$

Then it is clear that $J_s(mx, x) \approx J_s(0, \infty)$ for $mx < y_{s-}$ and $x > y_{s+}$. That is, essentially pure power law spectra obtain for values of x that lie between $x_{s\,\mathrm{min}}$ and $x_{s\,\mathrm{max}}$, where

$$x_{s\,\mathrm{min}} \approx y_{s+}, \qquad x_{s\,\mathrm{max}} \approx y_{s-/m}. \tag{45}$$

If $x < x_{s\,\mathrm{min}}$ or $x > x_{s\,\mathrm{max}}$, the dependence of the spectra departs significantly from that of a power law. Note $(x_{\mathrm{min}}, x_{\mathrm{max}})$ for $\Phi^T(K)$ are in general different than for Φ^v_{ij}, because s is different for the two cases for $P_T = P_v$, and/or because the $\tilde{B}(y)$ may be different. Also note that if $x_{s\,\mathrm{min}} \geq x_{s\,\mathrm{max}}$ in equation (45), then there is no inertial range.

2.4 Morphology Dependence

It is important to examine the effects of changing the envelope functions $\tilde{B}^2(y)$ that appear in the integrals $J_s(mx, x)$ of equation (38).

We may change an envelope function in several ways. One way is merely to alter its amplitude. But that is trivial, because the previous values of the functions $\Phi^T(K), \Phi^v_{ij}(K)$ could be maintained by commensurately altering the unknown amplitudes in equations (35) and (36).

Another way is to replace $\tilde{B}(y)$ by the same functions of a "stretched" argument, $\tilde{B}(y) \to \tilde{B}(\alpha y)$. This is equivalent to changing the spectrum of scale lengths in the ensemble, such that $a_\alpha \to a'_\alpha = \alpha a_\alpha$, and altering $(\delta T_1, v_1)$ appropriately to keep the same values of $\Phi^T(K), \Phi^v_{ij}(K)$ in the inertial range. But the boundaries of the inertial range will be shifted; that is, from equation (45), we get

$$K'_{p\,\mathrm{min}} = y_{p+}/a'_\alpha = K_{p\,\mathrm{min}}/\alpha, \qquad K'_{p\,\mathrm{max}} = K_{p\,\mathrm{max}}/\alpha. \tag{46}$$

Outside the inertial range, the spectra will be changed.

Another way is to replace a chosen $\tilde{B}(y)$ by a different functional form $\tilde{B}'(y)$. Clearly, this will change the boundaries of the inertial ranges, in general, but inside the inertial ranges, $(\delta T_1, v_1)$ can be altered to preserve the previous values of the spectra.

Therefore, we may conclude the following: the power law spectra in the inertial ranges are completely insensitive to all changes in turbule morphology, that is, alterations of the envelope functions $\tilde{B}(y)$. Changes in the spectrum of scale lengths and/or in the functional form (morphology) of the $\tilde{B}(y)$ irreducibly influence only the boundaries $(K_{p\,\mathrm{min}}, K_{p\,\mathrm{max}})$ of the inertial range and the behavior of $\Phi^T(K), \Phi^v_{ij}(K)$ outside the inertial range.

We will provide graphs of numerical examples in section 2.4.3.

2.4.1 Kolmogorov Spectra

From experimental and scaling considerations [4], the power law part of the spectrum is expected to go like $x^{-11/3}$, so $P = 11/3$. If this dependence were valid for all x, the spectral densities would be said to exhibit the "Kolmogorov spectrum."

From equations (42) and (17), this requires

$$\nu = 1/3 - q, \qquad \beta = 3(1-q). \tag{47}$$

We know that $q \geq 0$, since we insisted that a_α get smaller as α increases. Also, we expect that N_α increases as the scale length decreases; from equations (11) and (47), this requires $q < 1$. It is especially interesting to note that, for the fractal scaling ($q = 0$), which is often assumed [2], equation (47) yields

$$\nu = 1/3 \qquad \beta = 3. \tag{48}$$

The $\nu = 1/3$ result follows from the usual energy cascade model, upon requirement that the kinetic energy transfer rate *per unit mass* be independent of scale length [4]. The usual cascade model does not consider the number of eddies of each scale length, in contrast to our model of section 2.2. It is remarkable that only with fractal scaling does our model yield not only $\nu = 1/3$, but also $\beta = 3$, which corresponds to turbule packing fractions $N_\alpha a_\alpha^3/V_s$ independent of scale length.

The standard structure function description of isotropic homogeneous fully developed turbulence finds by dimensional analysis that the temperature and velocity structure functions of the turbulence must be given by

$$D_T(r) \equiv \left\langle \left(T_0(\mathbf{r}_1) - T_0(\mathbf{r}_2)\right)^2 \right\rangle = C_T^2 r^{2/3}, \tag{49}$$

$$D_{vrr}(r) \equiv \hat{r}_i \hat{r}_j \left\langle \left(v_{0i}(\mathbf{r}_1) - v_{0i}(\mathbf{r}_2)\right) \left(v_{0j}(\mathbf{r}_1) - v_{0j}(\mathbf{r}_2)\right) \right\rangle = C_v^2 r^{2/3}, \tag{50}$$

where

$$\mathbf{r} \equiv \mathbf{r}_1 - \mathbf{r}_2, \qquad r = |\mathbf{r}|, \qquad \hat{r} = \mathbf{r}/r, \tag{51}$$

and (C_T^2, C_v^2) are the so-called structure parameters. These are valid for some range of r called the "inertial range" between the inner and outer scale lengths (a_{N_s}, a_1). Assuming (incorrectly, of course) that these forms are valid for all r, the following spectral densities are easily derived:

$$\Phi^T(K) = 8.19\, C_T^2 V_s K^{-11/3} \tag{52}$$
$$\Phi_{ij}^v(K) = (\delta_{ij} - \hat{K}_i \hat{K}_j)(15.0\, C_v^2 V_s K^{-11/3}). \tag{53}$$

It is clear that these are incorrect for $K \to 0$, but they are valid for most K. Comparing these forms with equations (35) and (36), putting $P_T = P_v = 11/3$, neglecting $|\tilde{p}(\mathbf{K})|^2 << 1$ for K not near 0, and taking the values of the integrals of equation (33), in the inertial range of K, we get the following expressions for the structure parameters:

$$C_T^2 = (3.78/\mu)(N_1 a_1^3/V_s)(\delta T_1/a_1^{1/3})^2 J_{8/3}^T(0,\infty), \tag{54}$$
$$C_v^2 = (0.69/\mu)(N_1 a_1^3/V_s)(v_1/a_1^{1/3})^2 J_{14/3}^v(0,\infty). \tag{55}$$

Thus we have connected the structure parameters that are believed to characterize the Kolmogorov spectrum of isotropic homogeneous turbulence to the parameters of our scaled self-similar turbule model, an essential step. Note that for fractal scaling ($q = 0$), the factor $(N_1 a_1^3/V_s)$ may be replaced by $(N_\alpha a_\alpha^3/V_s)$ for any scale length α, and so may the factors $(\delta T_1/a_1^{1/3}, v_1/a_1^{1/3})$. This is not the case for $q \neq 0$.

2.4.2 Quasi-Gaussian Spectrum

Gaussian spectra involving a single scale length have been used fairly often [5,6]; we illustrate this for an isotropic ensemble of turbules of a given scale length in Goedecke et al [1]. It is interesting to note that our turbule ensemble model, containing many scale lengths, allows spectra for $\Phi^T(K), \Phi_{ij}^v(K)$ that are Gaussian for most K, for special choices of the envelope function $(\tilde{B}_T^2, \tilde{B}_v^2)$. In particular, if in equations (35) and (36) we put

$$P_T = P_v = 0, \qquad \tilde{B}_T^2(y) = y^2 e^{-y^2/2}, \qquad \tilde{B}_v^2(y) = e^{-y^2/2}, \tag{56}$$

we get

$$\Phi^T(K) = (1 - |\tilde{p}(K)|^2)(\text{constant})(e^{-m^2x^2/2} - e^{-x^2}), \tag{57}$$
$$\Phi_{ij}^v(K) = (\delta_{ij} - \hat{K}_i \hat{K}_j)(\text{constant})(e^{-m^2x^2/2} - e^{-x^2}). \tag{58}$$

For $K \to 0$ and for $K \to \infty$, these go to zero, as they should; but, for $x = Ka_1 >> 1$, they go to simple Gaussians involving the inner scale length a_{N_s}, since $mx = Ka_{N_s}$. These are a special case of a power law spectrum with $P = 0$ for the "inertial range" of K, that is, for $mx << 1$ and $x >> 1$.

From equations (17) and (39), the scaling exponents must then satisfy

$$\beta = 14 - 3q > 0, \qquad \nu = \gamma = 4 - q. \tag{59}$$

If we were to choose $\nu = 1/3$ as in the Kolmogorov spectrum with fractal scaling, this again yields $\beta = 3$, but requires $q = 11/3$, a rather steep power law for the length scales in the ensemble (see equation (14)).

2.4.3 Examples

It is important to give some examples using specific envelope functions, in order to illustrate some of the results of the last several sections. We will do this for the (quasi) Kolmogorov spectra, having dependence $x^{-11/3}$ in the inertial range.

In Goedecke et al [1], we considered two example envelope functions, a Gaussian and the Fourier transform of an exponential:

$$\tilde{B}_g^2(y) = e^{-y^2/2}, \qquad \tilde{B}_e^2(y) = (1 + y^2/12)^{-6}. \tag{60}$$

The factor 12 in $\tilde{B}_e^2(y)$ ensures that turbules of the same scale length have the same RMS radius [1]. For $P = 11/3$, we consider the normalized spectral densities

$$F_T(x) = x^{-11/3} J_{8/3}(mx, x)/J_{8/3}(0, \infty), \tag{61}$$
$$F_v(x) = x^{-11/3} J_{14/3}(mx, x)/J_{14/3}(0, \infty), \tag{62}$$

in which we use the same $\tilde{B}(y)$ for both temperature and velocity spectra, for convenience. These functions are the factors in equations (35) and (36) that determine the boundaries of the inertial ranges of K and the behavior of $\Phi^T(K)$, $\Phi_{ij}^v(K)$ outside the inertial ranges.

From equation (38), we have

$$J_s^g(mx, x) = \int_{mx}^{x} dy\, y^s e^{-y^2/2}, \tag{63}$$
$$J_s^e(mx, x) = \int_{mx}^{x} dy\, y^s (1 + y^2/12)^{-6}. \tag{64}$$

These integrals were evaluated for $s = (8/3, 14/3)$, for $m = (10^{-3}, 10^{-4})$, which are realistic values for the ratio a_N/a_1 of inner to outer scale length. That is, inner scale lengths may be of the order of millimeters, while outer scale lengths may be of the order of tens to hundreds of meters.

Figures 1 and 2 are plots of $\log F_T^g$ and $\log F_T^e$ versus $\log x$ for $m = 10^{-3}$ and 10^{-4}, respectively; figures 3 and 4 are plots of $\log F_v^g$ and $\log F_v^e$

Figure 1. Normalized isotropic homogeneous ensemble temperature spectra for $m = 10^{-3}$ as functions of outer scale size parameter ka_1.

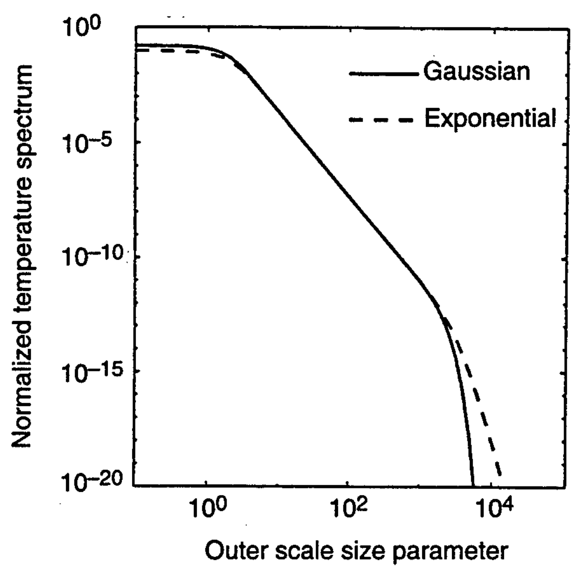

Figure 2. Normalized isotropic homogeneous ensemble temperature spectra for $m = 10^{-4}$ as functions of outer scale size parameter ka_1.

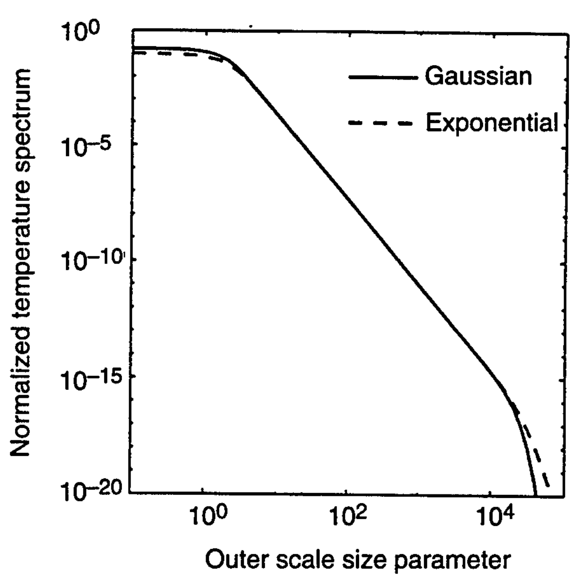

versus $\log x$ for $m = 10^{-3}$ and 10^{-4}, respectively. The plots, of course, coincide in the common portions of their inertial ranges; as discussed earlier, this coincidence can always be achieved for the actual spectra, for any choices of the envelope functions, by adjusting the (unknown) parameters $(\delta T_1, v_1)$. But the exponential and Gaussian envelopes yield slightly different inertial range boundaries, quite different behavior for $x > x_{s\,\max}$, and the same behavior but different values for $x < x_{s\,\min}$.

Figure 3. Normalized isotropic homogeneous ensemble velocity spectra for $m = 10^{-3}$ as functions of outer scale size parameter ka_1.

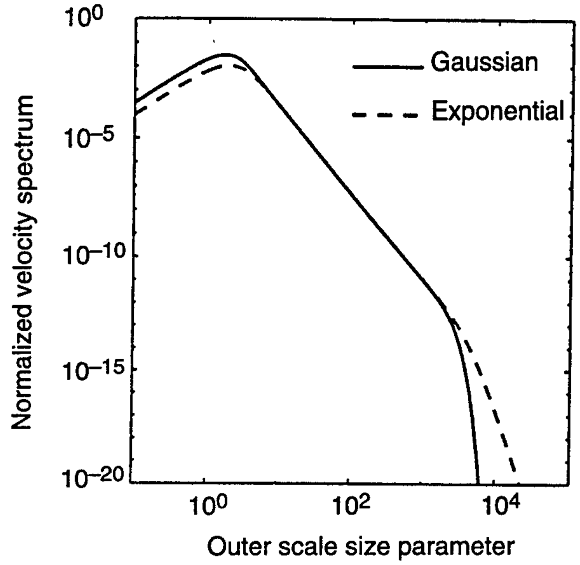

Figure 4. Normalized isotropic homogeneous ensemble velocity spectra for $m = 10^{-4}$ as functions of outer scale size parameter ka_1.

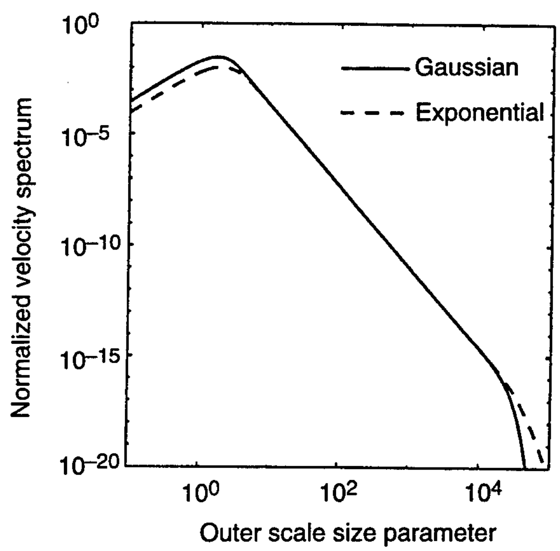

We may use the results of section 2.3.3 to estimate the inertial range boundaries, and compare the estimates with figures 1 to 4. Using equations (43) and (60), we get

$$y^g_{sm} = s^{1/2}, \qquad y^e_{sm} = s^{1/2}/(1-s/12)^{1/2} \tag{65}$$

for the (Gaussian, exponential) envelopes, respectively. Then by numerical solution of equation (44), using equation (45), we obtain the following inertial range boundaries for the temperature spectra, with $s = 8/3$:

$$x^g_{\min} \approx 3.19, \qquad x^g_{\max} \approx 0.49/m \tag{66}$$

$$x^e_{\min} \approx 4.45, \qquad x^e_{\max} \approx 0.52/m. \tag{67}$$

For the velocity spectra, with $s = 14/3$, the corresponding boundaries are

$$x^g_{\min} \approx 3.70, \qquad x^g_{\max} \approx 0.94/m \tag{68}$$

$$x^e_{\min} \approx 6.34, \qquad x^e_{\max} \approx 1.08/m. \tag{69}$$

These results compare reasonably well with the boundaries apparent in figures 1 to 4.

Based on the discussion in section 2.4, if we stretch the argument of the envelope functions ($\tilde{B}(y) \rightarrow \tilde{B}(\alpha y)$) or, equivalently, change the length scales ($a_\alpha \rightarrow \alpha a_\alpha$), then the boundaries ($K_{\min}, K_{\max}$) of the inertial ranges of K change according to equation (46). That is, if we knew or assumed a value of a_1, then we would get from $x = Ka_1$ and equation (66)

$$K^g_{\min} \approx 3.19/a_1, \qquad K^g_{\max} \approx 0.49/ma_1 = 0.49/ma_{N_s} \tag{70}$$

and similarly from equations (67) and (69). If we then change a_1 by $a_1 \rightarrow \alpha a_1$, we get

$$K^g_{\min} \approx 3.19/\alpha a_1 = K^g_{\min}/\alpha, \text{ etc.} \tag{71}$$

3. Acoustic Scattering

For an isotropic homogeneous turbulence in a volume V_T, the far-field Born approximation differential cross-section for scattering of an acoustic plane wave is given by [4]

$$\bar{\sigma}(\hat{\mathbf{r}}) = \bar{\sigma}_T(\hat{\mathbf{r}}) + \bar{\sigma}_v(\hat{\mathbf{r}}), \tag{72}$$

where

$$\bar{\sigma}_T(\hat{\mathbf{r}}) = (k^2/4\pi T_\infty)^2 \cos^2\theta \Phi^T(K) \tag{73}$$
$$\bar{\sigma}_v(\hat{\mathbf{r}}) = (k^2/2\pi c_\infty)^2 \cos^2\theta \hat{k}_i \hat{k}_j \Phi^v_{ij}(K); \tag{74}$$

and here,

$$\mathbf{K} \equiv k\hat{\mathbf{r}} - \hat{\mathbf{k}}, \qquad K = |\mathbf{K}| = 2k\sin(\theta/2), \tag{75}$$

where $\hat{\mathbf{r}}$ is the observation direction, $\hat{\mathbf{k}}$ is the incident plane wave propagation vector, with $k = 2\pi/\lambda$, $\lambda =$ wavelength, θ is the scattering angle, the angle between $\hat{\mathbf{r}}$ and $\hat{\mathbf{k}}$, $0 \le \theta \le \pi$, and $\Phi^T(K)$ and $\Phi^v_{ij}(K)$ are the spectra of the turbulent temperature variations and velocity, respectively, given by equations (35) and (36). In equation (73), T_∞ is the reference temperature outside the volume V_T, which has been chosen equal to the mean temperature inside V_T, as discussed in the previous section. In equation (74), we have

$$\hat{k}_i \hat{k}_j \Phi^v_{ij}(\mathbf{K}) = \hat{k}_i \hat{k}_j \left(\delta_{ij} - \hat{K}_i \hat{K}_j\right) G_v(K) = \cos^2(\theta/2) G_v(K), \tag{76}$$

where, from equation (36),

$$G_v(K) = (\pi^3 N_1 v_1^2 a_1^6 / 3\mu) x^{-P_v} J^v_{P_v+1}(mx, x), \tag{77}$$

and from equations (37) and (75)

$$x = Ka_1 = 2ka_1 \sin(\theta/2). \tag{78}$$

Equations (73) and (74) are valid for cases in which V_T is the scattering volume V_s, or in which $V_s < V_T$, but the scale length a_s of V_s satisfies

$a_s >> a_\alpha$, as discussed by Goedecke et al [1], and in equations (35) and (36), N_1 is the mean number of turbules of scale length a_1 in V_s.

The cross-sections in equations (73) and (74) are thus proportional to the normalized spectral densities in equations (61) and (62), and figures 1 to 4 therefore reveal the crucial behavior of the scattering cross-sections $\bar{\sigma}_T(\hat{\mathbf{r}}),\ \bar{\sigma}_v(\hat{\mathbf{r}})$ for the sample envelope function considered in section 2.4.3, except for the factors of $\cos^2\theta$ and $\cos^2\theta\cos^2(\theta/2)$. It is important to note that here, the boundaries of the inertial range of x or K translate into boundaries of the inertial range of scattering angles $(\theta_{\min}, \theta_{\max})$. For example, for the Gaussian envelope function and the $x^{-11/3}$ power law in the inertial range, we have from equation (66) the temperature scattering

$$\sin(\theta_{\min}/2) \approx (3.19)/(2ka_1), \qquad \sin(\theta_{\max}/2) \approx (0.49)(2mka_1). \qquad (79)$$

Clearly, $\sin(\theta/2) \leq 1$ for $0 \leq \theta \leq \pi$. So, if mka_1 is less than or approximately equal to 0.25, the upper inertial range boundary is never reached; that is, the power law spectrum obtains for scattering angles out to $\theta = \pi$.

For example, suppose the following reasonable values are chosen: $m = 10^{-4}, a_1 = 10^2 m, \lambda = 0.314m \rightarrow k \approx 20m^{-1}, ka \approx 2 \times 10^3$. Then, from equation (79)

$$\sin(\theta_{\min}/2) \approx 1.6 \times 10^{-3}, \qquad \sin(\theta_{\max}/2) \approx 2.5. \qquad (80)$$

So the power law spectrum would obtain for almost all angles; the effect of the factor $1 - |\tilde{p}(\mathbf{K})|^2$ in $\Phi^T(K)$ might dominate at angles as small as this $\theta_{\min}$. If ka_1 were much smaller, then $\theta_{\min}$ would be observable, but not $\theta_{\max}$; if ka_1 were larger, then $\theta_{\max}$ would be observable in principle, but $\theta_{\min}$ would be too small to be observed.

4. Summary and Discussion

In this report, we have established that a self-similar ensemble of localized stationary turbules of arbitrary morphology and many different scale lengths, but with random orientations and locations within a volume V_s, predict spectral densities ($\Phi^T(K), \Phi^v_{ij}(K)$) of the temperature and velocity structure functions of the turbulence that have the following properties:

1. The spectra obey power laws (K^{-P_T}, K^{-P_v}) in ranges $K_{\min} \leq K \leq K_{\max}$, conventionally called the inertial ranges, which may be different for $\Phi^T(K)$ than for $\Phi^v_{ij}(K)$. The values (P_T, P_v) are determined by choices of scaling exponents, and are independent of turble morphology, as are the values of the spectral densities in the inertial range. The boundaries ($K_{\min}, K_{\max}$) of the inertial range and the behavior of the spectral densities for K outside the inertial range are sensitive to turbule morphology.
2. The choice $P_T = P_v = 11/3$, corresponding to the Kolmogorov spectrum with a fractal size scaling $a_{\alpha+1}/a_\alpha$ = constant, yields the usual scaling relation $v_\alpha a_\alpha^{1/3}$ = constant, and also requires that packing fractions of turbules in V_s are independent of scale length. Expressions for the structure parameters (C_T^2, C_v^2) of the Kolmogorov spectra were obtained in terms of turbule model parameters.
3. The choice $P_v = P_T = 0$ yields a quasi-Gaussian spectrum for a Gaussian ensemble average turbule morphology.
4. The first Born approximation far-field acoustic scattering cross-sections due to the turbulent temperature and velocity fluctuations exhibit a power law dependence $(\sin\theta/2)^{-P_T}$, $(\sin\theta/2)^{-P_v}$ in inertial ranges $\theta_{\min} \leq \theta \leq \theta_{\max}$ determined by ($K_{\min}, K_{\max}$), but deviate markedly from this dependence for scattering angles θ outside the inertial ranges. Depending primarily on the values of the acoustic wavelength and the outer and inner scale lengths of the turbulence, these deviations may not be observable in practice, because the power law may be valid from very small angles out to $\theta = 180°$.

There is quite a bit more that can be done with turbule models of atmospheric turbulence. For example, treatment of cases in which the mean temperature in V_s is not equal to the background reference temperature can be done; this will yield a different power law for $\Phi^T(K)$ for small K than for large K. Also, consideration should be given to situations that must often occur in practice, in which the scattering volume V_s is smaller than some of the large-scale turbules, and/or the observation distance is not in the far field of V_s. These situations may change the results significantly. They will also be considered in future reports.

The ultimate goal of the research reported in this series of reports is to describe acoustic scattering and propagation in anisotropic and/or inhomogeneous turbulence. It is hoped that a turbule approach will be particularly appropriate for this description.

References

1. G. H. Goedecke, M. DeAntonio, and H. J. Auvermann, *First-Order Wave Equations and Scattering by Atmospheric Turbules*, U.S. Army Research Laboratory, ARL-TR-1356 (August 1997).
2. A. S. Monin, "Characteristics of the Scattering of Sound in a Turbulent Atmosphere," *Sov. Phys. Acoust.* **7**, 130 (1962).
3. M. Nelkin, "In what sense is turbulence an unsolved problem?," *Science* **255**, 566–570 (1992).
4. V. I. Tatarskii, *The Effects of the Turbulent Atmosphere on Wave Propagation*, chap. 2, Keter, Jerusalem (1971).
5. W. E. McBride, H. E. Bass, R. Raspet, and K. E. Gilbert, "Scattering of sound by atmospheric turbulence: Predictions in a refractive shadow zone," *J. Acoust. Soc. Am.* **91**, 1336–1340 (1992).
6. V. Ostashev, V. Mellert, R. Wandelt, and F. Gerdes, "Sound propagation in moving random media with the Gaussian correlation function of medium inhomogeneities. I. Plane wave propagation," accepted for publication in *J. Acoust. Soc. Am.* (1997).

Distribution

Admnstr
Defns Techl Info Ctr
Attn DTIC-OCP
8725 John J Kingman Rd Ste 0944
FT Belvoir VA 22060-6218

Mil Asst for Env Sci
Ofc of the Undersec of Defns for Rsrch &
Engrg R&AT E LS
Pentagon Rm 3D129
Washington DC 20301-3080

Ofc of the Secy of Defns
Attn ODDRE (R&AT)
Attn ODDRE (R&AT) S Gontarek
The Pentagon
Washington DC 20301-3080

Army ARDEC
Attn SMCAR-IMI-I
Bldg 59
Dover NJ 07806-5000

Army Communications Elec Ctr
for EW RSTA
Attn AMSEL-EW-D
Attn AMSEL-EW-MD
FT Monmouth NJ 07703-5303

Army Corps of Engrs
Engr Topographics Lab
Attn ETL-GS-LB
FT Belvoir VA 22060

Army Dugway Proving Ground
Attn STEDP 3
Dugway UT 84022-5000

Army Field Artillery School
Attn ATSF-TSM-TA
FT Sill OK 73503-5000

Army Foreign Sci Tech Ctr
Attn CM
220 7th St NE
Charlottesville VA 22901-5396

Army Infantry
Attn ATSH-CD-CS-OR E Dutoit
FT Benning GA 30905-5090

Army Nuclear CML Agency
Attn MONA ZB
Bldg 2073
Springfield VA 22150-3198

Army OEC
Attn CSTE EFS
4501 Ford Ave Park Center IV
Alexandria VA 22302-1458

Army Rsrch Ofc
Attn AMXRO-GS Bach
PO Box 12211
Research Triangle Park NC 27709

Army Satellite Comm Agcy
Attn DRCPM-SC-3
FT Monmouth NJ 07703-5303

Army Strat Defns Cmnd
Attn CSSD-SL-L Lilly
PO Box 1500
Huntsville AL 35807-3801

CECOM
Attn PM GPS COL S Young
FT Monmouth NJ 07703

CECOM
Sp & Terrestrial Commctn Div
Attn AMSEL-RD-ST-MC-M H Soicher
FT Monmouth NJ 07703-5203

DARPA
Attn B Kaspar
Attn L Stotts
3701 N Fairfax Dr
Arlington VA 22203-1714

Dir of Assessment and Eval
Attn SARD-ZD H K Fallin Jr
103 Army Pentagon Rm 2E673
Washington DC 20310-0163

Hdqtrs Dept of the Army
Attn DAMO-FDT D Schmidt
400 Army Pentagon Rm 3C514
Washington DC 20310-0460

Distribution (cont'd)

MICOM RDEC
Attn AMSMI-RD W C McCorkle
Redstone Arsenal AL 35898-5240

Natl Security Agency
Attn W21 Longbothum
9800 Savage Rd
FT George G Meade MD 20755-6000

Naval Air Dev Ctr
Attn Code 5012 A Salik
Warminister PA 18974

OSD
Attn OUSD(A&T)/ODDDR&E(R) R Trew
The Pentagon
Washington DC 20301-7100

Science & Technology
101 Research Dr
Hampton VA 23666-1340

US Army Avn Rsrch, Dev, & Engrg Ctr
Attn T L House
4300 Goodfellow Blvd
St Louis MO 63120-1798

US Army Edgewood Rsrch, Dev, & Engrg Ctr
Attn SCBRD-TD J Vervier
Aberdeen Proving Ground MD 21010-5423

US Army Info Sys Engrg Cmd
Attn ASQB-OTD F Jenia
FT Huachuca AZ 85613-5300

US Army Materiel Sys Analysis Agency
Attn AMXSY-D J McCarthy
Aberdeen Proving Ground MD 21005-5071

US Army Mis Cmnd (USAMICOM)
Attn AMSMI-RD-CS-R Documents
Redstone Arsenal AL 35898-5400

US Army Natick Rsrch, Dev, & Engrg Ctr
Acting Techl Dir
Attn SSCNC-T P Brandler
Natick MA 01760-5002

Dir US Army Rsrch Ofc
4300 S Miami Blvd
Research Triangle Park NC 27709

US Army Simulation, Train, & Instrmntn Cmd
Attn J Stahl
12350 Research Parkway
Orlando FL 32826-3726

US Army Tank-Automtv & Armaments Cmd
Attn AMSTA-AR-TD C Spinelli
Bldg 1
Picatinny Arsenal NJ 07806-5000

US Army Tank-Automtv Cmd Rsrch, Dev, & Engrg Ctr
Attn AMSTA-TA J Chapin
Warren MI 48397-5000

US Army Test & Eval Cmd
Attn R G Pollard III
Aberdeen Proving Ground MD 21005-5055

US Army TRADOC Anlys Cmnd WSMR
Attn ATRC-WSS-R
White Sands Missile Range NM 88002

US Army Train & Doctrine Cmd
Battle Lab Integration & Techl Dirctrt
Attn ATCD-B J A Klevecz
FT Monroe VA 23651-5850

US Military Academy
Dept of Mathematical Sci
Attn MAJ D Engen
West Point NY 10996

USACRREL
Attn CEREL-GP R Detsch
72 Lyme Rd
Hanover NH 03755-1290

USATRADOC
Attn ATCD-FA
FT Monroe VA 23651-5170

Nav Air War Cen Wpn Div
Attn CMD 420000D C0245 A Shlanta
1 Admin Cir
China Lake CA 93555-6001

Nav Ocean Sys Ctr
Attn Code 54 Richter
San Diego CA 92152-5000

Distribution (cont'd)

Nav Surface Warfare Ctr
Attn Code B07 J Pennella
17320 Dahlgren Rd Bldg 1470 Rm 1101
Dahlgren VA 22448-5100

Naval Surface Weapons Ctr
Attn Code G63
Dahlgren VA 22448-5000

AFMC DOW
Wright Patterson AFB OH 45433-5000

Air Weather Service
Attn Tech Lib FL4414 3
Scott AFB IL 62225-5458

GPS Joint Prog Ofc Dir
Attn COL J Clay
2435 Vela Way Ste 1613
Los Angeles AFB CA 90245-5500

Ofc of the Dir Rsrch and Engrg
Attn R Menz
Pentagon Rm 3E1089
Washington DC 20301-3080

Phillips Lab Atmospheric Sci Div
Geophysics Dirctrt
Hanscom AFB MA 01731-5000

USAF Rome Lab Tech
Attn Corridor W Ste 262 RL SUL
26 Electr Pkwy Bldg 106
Griffiss AFB NY 13441-4514

NASA Marshal Space Flt Ctr
Atmospheric Sciences Div
Attn E501 Fichtl
Huntsville AL 35802

NASA Spct Flt Ctr Atmospheric Sciences Div
Attn Code ED 41 1
Huntsville AL 35812

ARL Electromag Group
Attn Campus Mail Code F0250 A Tucker
University of Texas
Austin TX 78712

Hicks & Associates, Inc.
Attn G Singley
1710 Goodrich Dr Ste 1300
McLean VA 22102

Dir for MANPRINT
Ofc of the Deputy Chief of Staff for Prsnnl
Attn J Hiller
The Pentagon Rm 2C733
Washington DC 20310-0300

Lockheed Missile & Spc Co
Attn Org 91 01 B 255 K R Hardy
3251 Hanover St
Palo Alto CA 94304-1191

Natl Ctr for Atmospheric Research
Attn NCAR Library Serials
PO Box 3000
Boulder CO 80307-3000

NCSU
Attn J Davis
PO Box 8208
Raleigh NC 27650-8208

New Mexico State University
Dept of Physics
Attn G Goedecke (5 copies)
Las Cruces, NM 88003-8001

NTIA ITS S3
Attn H J Liebe
325 S Broadway
Boulder CO 80303

Pacific Missile Test Ctr Geophysics Div
Attn Code 3250
Point Mugu CA 93042-5000

Army Rsrch Lab
Attn AMSRL-IS-EW
White Sands Missile Range NM 88002-5501

Distribution (cont'd)

US Army Rsrch Lab
Attn AMSRL-CI-LL Techl Lib (3 copies)
Attn AMSRL-CS-AL-TA Mail & Records Mgmt
Attn AMSRL-CS-AL-TP Techl Pub (3 copies)
Attn AMSRL-IS-EE H J Auvermann (10 copies)
Adelphi MD 20783-1197

REPORT DOCUMENTATION PAGE

Form Approved
OMB No. 0704-0188

1. AGENCY USE ONLY *(Leave blank)*	2. REPORT DATE	3. REPORT TYPE AND DATES COVERED
	August 1998	Interim, from Mar 1991 to Dec 1994

4. TITLE AND SUBTITLE
Structure Function Spectra and Acoustic Scattering Due to Homogeneous Isotropic Atmospheric Turbule Ensembles

5. FUNDING NUMBERS
PE: 62784A
DA PR: AH71

6. AUTHOR(S)
George H. Goedecke, Michael DeAntonio (New Mexico State Univ), and Harry J. Auvermann (ARL)

7. PERFORMING ORGANIZATION NAME(S) AND ADDRESS(ES)
U.S. Army Research Laboratory
Attn: AMSRL-IS-EE (hauverma@arl.mil)
2800 Powder Mill Road
Adelphi, MD 20783-1197

8. PERFORMING ORGANIZATION REPORT NUMBER
ARL-TR-1518

9. SPONSORING/MONITORING AGENCY NAME(S) AND ADDRESS(ES)
U.S. Army Research Laboratory
2800 Powder Mill Road
Adelphi, MD 20783-1197

10. SPONSORING/MONITORING AGENCY REPORT NUMBER

11. SUPPLEMENTARY NOTES
AMS code: 622784H7111
ARL PR: 8HEF50

12a. DISTRIBUTION/AVAILABILITY STATEMENT
Approved for public release; distribution unlimited.

12b. DISTRIBUTION CODE

13. ABSTRACT *(Maximum 200 words)*

Expressions are derived for the spectral densities $\Phi^T(K),\Phi_{ij}^v(K)$ of the temperature and velocity structure functions of atmospheric turbulence, and for the corresponding Born approximation far-field acoustic scattering cross-sections, due to homogeneous isotropic stationary ensembles of self-similar localized turbules having many different scale lengths. It is shown that for some range $K_{min} \leq K \leq K_{max}$, the "inertial range," the spectral densities obey power laws with dependence K^{-P_T},K^{-P_v}. The exponents (P_T,P_v) depend only on choices of scaling relations and are independent of turbule morphology. Only K_{min}, K_{max}, and the values of the spectral densities outside the inertial range are morphology-dependent. Expressions for K_{min} and K_{max} are derived in terms of inner and outer scale lengths in the turbule ensemble. If the turbule scale lengths a_α are chosen to be in geometric sequence ($a_{\alpha+1}/a_\alpha$ = constant independent of α), and if the power law is given as $P_T = P_v = 11/3$, the Kolmogorov spectrum in the inertial range, then not only must the turbule velocity and temperature amplitudes scale as $a_\alpha^{1/3}$, the usual result, but also the turbule packing fractions must be independent of scale length. Expressions for the structure parameters (C_T^2,C_v^2) that occur in the usual Kolmogorov spectra are obtained in terms of the turbule model parameters. It is also shown that quasi-Gaussian spectra result for the choice $P_T = P_v = 0$ and Gaussian turbule morphology.

14. SUBJECT TERMS	15. NUMBER OF PAGES
Acoustic scattering, atmospheric turbulence	34
	16. PRICE CODE

17. SECURITY CLASSIFICATION OF REPORT	18. SECURITY CLASSIFICATION OF THIS PAGE	19. SECURITY CLASSIFICATION OF ABSTRACT	20. LIMITATION OF ABSTRACT
Unclassified	Unclassified	Unclassified	UL

NSN 7540-01-280-5500

Standard Form 298 (Rev. 2-89)
Prescribed by ANSI Std. Z39-18
298-102